

# Diachronous Tibetan Plateau landscape evolution derived from lava field geomorphology

Robert Law<sup>1,2</sup> and Mark B. Allen<sup>2</sup>

<sup>1</sup>Scott Polar Research Institute, Department of Geography, Cambridge University, Cambridge CB2 1ER, UK

<sup>2</sup>Department of Earth Sciences, Durham University, South Road, Durham DH1 3LE, UK

## ABSTRACT

Evolution of the Tibetan Plateau is important for understanding continental tectonics because of the plateau's exceptional elevation (~5 km above sea level) and crustal thickness (~70 km). Patterns of long-term landscape evolution can constrain tectonic processes, but have been hard to quantify, in contrast to established data sets for strain, exhumation, and paleo-elevation. This study analyzes the relief of the bases and tops of 17 Cenozoic lava fields on the central and northern Tibetan Plateau. Analyzed fields have typical lateral dimensions of tens of kilometers, and so have an appropriate scale for interpreting tectonic geomorphology. Fourteen of the fields have not been deformed since eruption. One field is cut by normal faults; two others are gently folded, with limb dips <6°. Relief of the bases and tops of the fields is comparable to that of modern, internally drained parts of the plateau, and distinctly lower than that of externally drained regions. The lavas preserve a record of underlying low-relief bedrock landscapes at the time they were erupted, which have undergone little change since. There is an overlap in each area between younger published low-temperature thermochronology ages and the age of the oldest eruption in each area, here interpreted as the transition between the end of significant (>3 km) exhumation and plateau landscape development. This diachronous process took place between ~32.5°N and ~36.5°N and between ca. 40 Ma and ca. 10 Ma, advancing northwards at a long-term rate of ~15 km/m.y. Results are consistent with incremental northward growth of the plateau, rather than a stepwise evolution or synchronous uplift.

## INTRODUCTION

This paper aims to determine time scales between the end of significant exhumation and the creation of relatively low-relief landscapes across the Tibetan Plateau (Figs. 1A and 1B), using lava fields as markers for the timing of deformation and landscape evolution (Fig. 1C). Study of the rise of the Tibetan Plateau to its present ~5 km elevation helps in understanding how continents deform in response to plate convergence. It is debated how northward convergence and plateau growth have taken place since initial collision of the Indian and Eurasian plates at ca. 60 Ma (Yin and Harrison, 2000; Kapp and DeCelles, 2019). Proposed mechanisms include stepwise continental subduction and crustal thickening within Tibet (Fig. 2A; Tapponnier et al., 2001) and incremental crustal shortening and thickening of Tibetan terranes to double normal crustal thickness (Fig. 2B; England and Houseman, 1986). Surface uplift is a conse-

quence of crustal shortening and thickening via isostasy, but other proposed mechanisms include: (1) mantle lithosphere detachment (Fig. 2C; England and Houseman, 1989), (2) crustal thickening as a consequence of lower-crustal flow (Fig. 2D; Clark and Royden, 2000), and (3) magmatic additions, possibly accompanying loss of the lower lithosphere (Fig. 2C; Chen et al., 2018). Combinations are possible; e.g., a component of lower-crustal flow could account for discrepancies between crustal shortening and present crustal thickness and surface elevations in northern Tibet (e.g., Staisch et al., 2016). There is also evidence for early Cenozoic exhumation near the present northern limits of the plateau (e.g., Liu et al., 2017). The schematic cross-sections in Figure 2 do not show this complexity.

Patterns of surface uplift and relief can constrain underlying processes, e.g., by distinguishing whether plateau growth is episodic with stepwise jumps in the location of marginal

fold-and-thrust belts (Fig. 2A; Tapponnier et al., 2001), incremental northward (Fig. 2B; England and Houseman, 1986), or synchronous across broad areas (Fig. 2C; England and Houseman, 1989).

Surface elevation has been addressed through  $\delta^{18}\text{O}$  isotope studies and paleobotany. Collective data sets indicate elevations of >4000 m as early as the Eocene in southern and central Tibet (e.g., Rowley and Currie, 2006; see Kapp and DeCelles [2019] for a summary). Low-temperature thermochronology data have been used to interpret exhumation histories, related to crustal thickening and consequent surface uplift (Jolivet et al., 2001; Wang et al., 2008; Rohrmann et al., 2012; McRivette et al., 2019), and show limited (<3 km) exhumation since 45 Ma in central Tibet (Rohrmann et al., 2012). However, neither paleo-elevation nor exhumation-rate data give direct information on topographic relief over time nor the development of landscapes similar to the modern plateau. Undeformed lower Miocene lacustrine rocks of the Wudaoliang Group cover much of central Tibet (Wu et al., 2008), indicating low relief, but such stratigraphic constraints are rare.

Collision-zone volcanic rocks have potential to track landscape development: flow bases record the underlying landscape at the time of eruption, while the upper surface acts as a marker for later deformation and incision (Wang et al., 2008). Volcanic centers that post-date initial India-Asia collision are widespread, if scattered, across the central and northern Tibetan Plateau (Ding et al., 2003; Chung et al., 2005; Wang et al., 2016; Chapman and Kapp, 2017; Kapp and DeCelles, 2019; Guo and Wilson, 2019; Yakovlev et al., 2019). Compositions are commonly potassic and ultrapotassic with some adakites, and crustal melt rhyolites in the north. Lava fields range in area from <100 to ~1000 km<sup>2</sup> with lateral extents typically of tens of kilometers (Table DR1 and Fig. DR1 in the

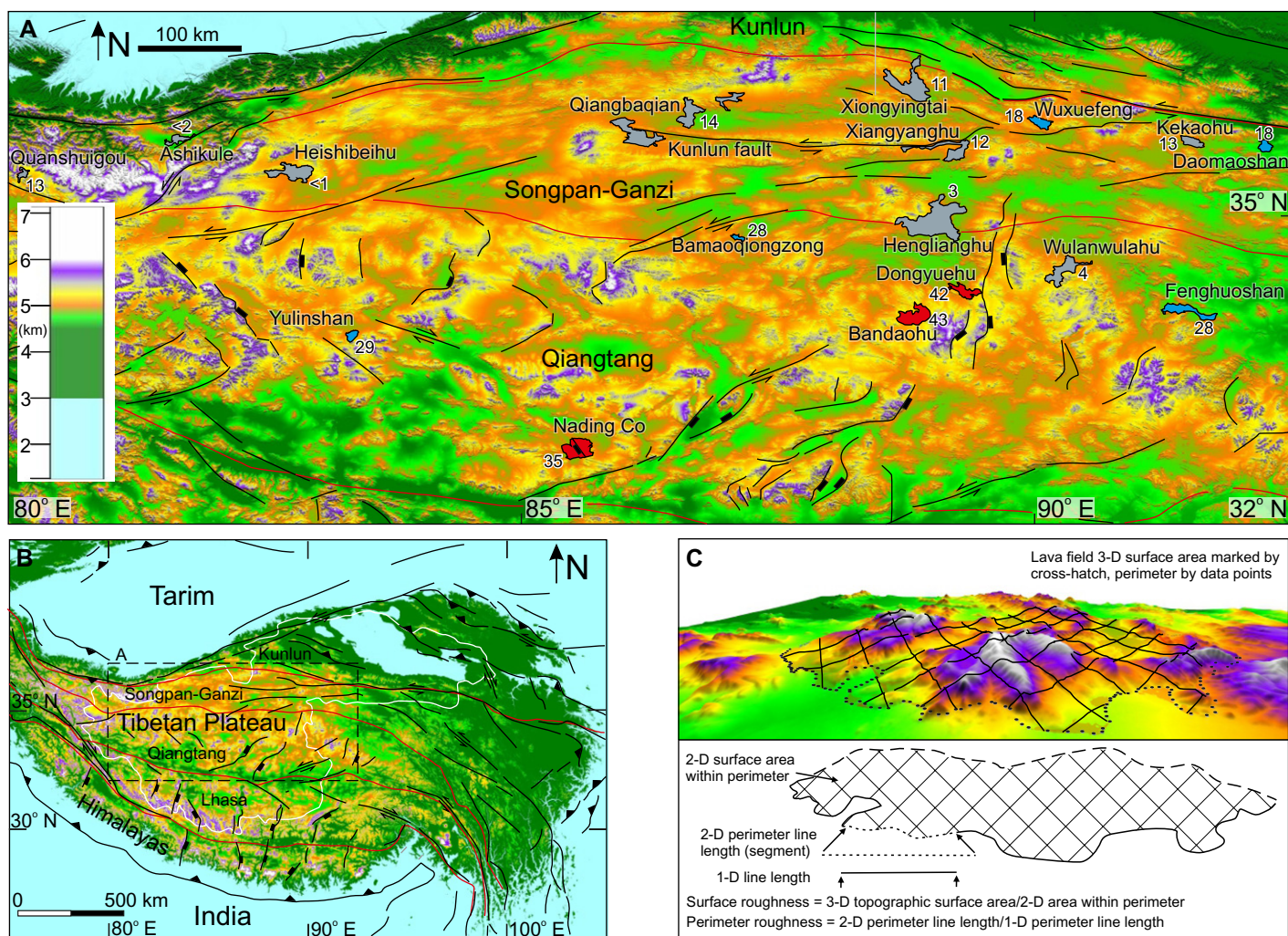


**Figure 1. Regional tectonics and topography of the Tibetan Plateau. (A) Location of lava fields in this study. Elevation color scale is scaled to emphasize internal plateau relief. Ages of lava fields are shown (in Ma); red color = 45–30 Ma, blue = 30–15 Ma, gray = 15–0 Ma. Active faults are from Taylor and Yin (2009); terrane boundaries in red. (B) Overview map of the Tibetan Plateau. Terrane boundaries (red) and internal drainage boundary of the plateau (white) are shown. Elevation scale is as for A. (C) Representation of surface roughness and perimeter roughness parameters. 1-D, 2-D, 3-D—one-, two-, three-dimensional.**

GSA Data Repository<sup>1</sup>). Accumulated flows are ~10–150 m thick (Guo et al., 2006).

Our approach is to first show that Tibetan Plateau lavas capped low-relief landscapes comparable to the modern plateau, with little erosion or deformation of fields since eruption. We then compare lava age distributions to published thermochronology data to explore time scales between the end of significant exhumation ( $\geq 3$  km) and creation of plateau landscapes. Age determinations have previously been used with geological data, such as unconformities, to interpret the end of deformation at a specific locality (Wang et al., 2008; Kapp and DeCelles, 2019); here we perform a regional study to understand landscape evolution across

the plateau, and test different models for tectonic evolution (Fig. 2).

## METHODS

We examined contacts and morphologies of lava fields using satellite imagery from Google Earth<sup>TM</sup>, Landsat, and digital topography (Shuttle Radar Topography Mission [SRTM] 1 arc-second data set; <https://www2.jpl.nasa.gov/srtm/>). Our study focuses on the Qiangtang and Songpan-Ganzi terranes of the central and northern Tibetan Plateau (32.5°–36.5°N, 88°–92°E; Fig. 1; Fig. DR1); this region contains the majority of lava fields in these terranes. The data set does not include every field, but focuses on fields large enough to yield meaningful results, i.e., with lateral dimensions of  $\geq 10$  km; these are on a length scale great enough to record regional deformation. Fifteen of the 17 flows analyzed in this study lie within the area of modern internal drainage (Fig. 1); the remaining two are just outside.

Contacts between lavas and underlying rocks were studied by profiling the elevation of the flow base around the present outcrop perimeters for 17 individual lava fields and compiling results as section lines. Perimeter roughness (PR) is defined as the ratio of the path along the topographic surface to the flat perimeter length. Higher values indicate higher-relief terrain, and areas with comparable tectonic and erosion histories would be expected to have similar PR values. Figure 1C shows the approach schematically. Results were compared with those from a random sample of 60 circular areas within the internally and externally drained parts of the plateau with perimeters of 100 km (Fig. DR2; Tables DR2 and DR3). Surface roughness (SR) was measured for the lava fields. SR is the ratio between the topographic surface of an area and the corresponding area of flat topography (Fig. 1C). Lava field data were compared with those from the random sample of areas.

<sup>1</sup>GSA Data Repository item 2020073, lava field and test area parameters (Tables DR1–DR3), is available online at <http://www.geosociety.org/datarepository/2020/>, or on request from [editing@geosociety.org](mailto:editing@geosociety.org).



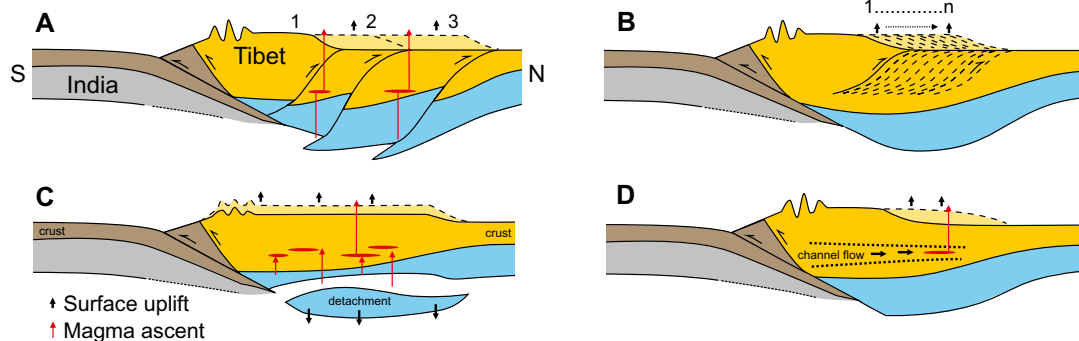


**Figure 2.** End-member tectonic models for growth of the Tibetan Plateau. (A) Northward stepwise growth involving crustal thickening above continental subduction (Tapponnier et al., 2001). (B) Incremental northward growth by lithospheric thickening (England and Houseman, 1986). (C) Rapid regional and synchronous surface uplift following removal of lower lithosphere, with accompanying magmatism (England and Houseman, 1989). (D) Crustal thickening, but not shortening, via lower-crustal flow (Clark and Royden, 2000).

Results were compared with published lava ages (Table DR1) and low-temperature thermochronologic data (apatite fission track and apatite [U-Th]/He analyses; Jolivet et al., 2001; Wang et al., 2008; Rohrmann et al., 2012). The thermochronologic ages indicate the time at which samples passed through the partial retention zone temperature window, and so constrain the timing of cooling and, indirectly, exhumation to within ~3 km of the surface. Using this combined approach, it is possible to track the end of significant exhumation, onset of extrusive magmatism, and landscape evolution history across a large area of the Tibetan Plateau, and to use these results to discriminate between different tectonic models (Fig. 2).

## RESULTS

The present-day interior of the Tibetan Plateau is rugged rather than completely flat, with relief commonly  $\leq 500$  m between summits and adjacent valleys and ~1 km across active fault

zones (Fig. 1). Lavas flowed over previously deformed bedrock, which had been eroded by the time of eruption (Fig. DR1). There is rarely an obvious relationship to major faults or fault-controlled basins; the Ashikule field is an exception. The great majority of fields (14 out of 17) appear to be unfaulted and unfolded since eruption (Fig. DR1). Three lava fields are deformed. Upper Miocene (ca. 12 Ma) lavas at Xiangyanghu (35.5°N, 89°E) are mildly deformed as part of a gentle west-east fold that lies parallel to the nearby Kunlun fault. The Kunlun fault is an active strike-slip fault, but has evidence for associated, localized, compressional deformation: e.g., there were west-east-striking thrust focal mechanisms in the aftermath of the A.D. 2001M 8 strike-slip earthquake, ~300 km east of Xiangyanghu (Ozacar and Beck, 2004). Oligocene (ca. 28–30 Ma) lava flows at Yulinshan (33.8°N, 83.3°E) are gently warped along an east-west axis, with a half-wavelength of ~10 km and a fold amplitude of ~250 m (Ding et al., 2003).

Both of these fields are dissected into discrete remnants by erosion, which is not the case for the other studied fields (Fig. DR1). Late Eocene (ca. 36 Ma) lavas at Nading Co (32.7°N, 85.5°E) are cut by normal faults (Ding et al., 2007); these faults are part of the middle Miocene–recent extensional fault system within the Tibetan Plateau (Taylor and Yin, 2009).

The lava fields' basal relief indicates landscapes comparable to internally drained parts of the modern plateau at the time of each eruption (Figs. 3A–3B): average (mean) PR values are 1.003 (maximum/minimum: 1.009/1.001) and 1.017 (1.044/1.003) for the lava fields and internally drained regions respectively (Tables DR1 and DR2). Both the lava fields and internally drained regions are distinctly different from externally drained regions in the east of the plateau (Fig. 3A), where relief is 1–2 km across major river gorges and average PR for the 30 test areas is 1.095 (1.205/1.006) (Table DR3). The lava fields show a similar mean SR

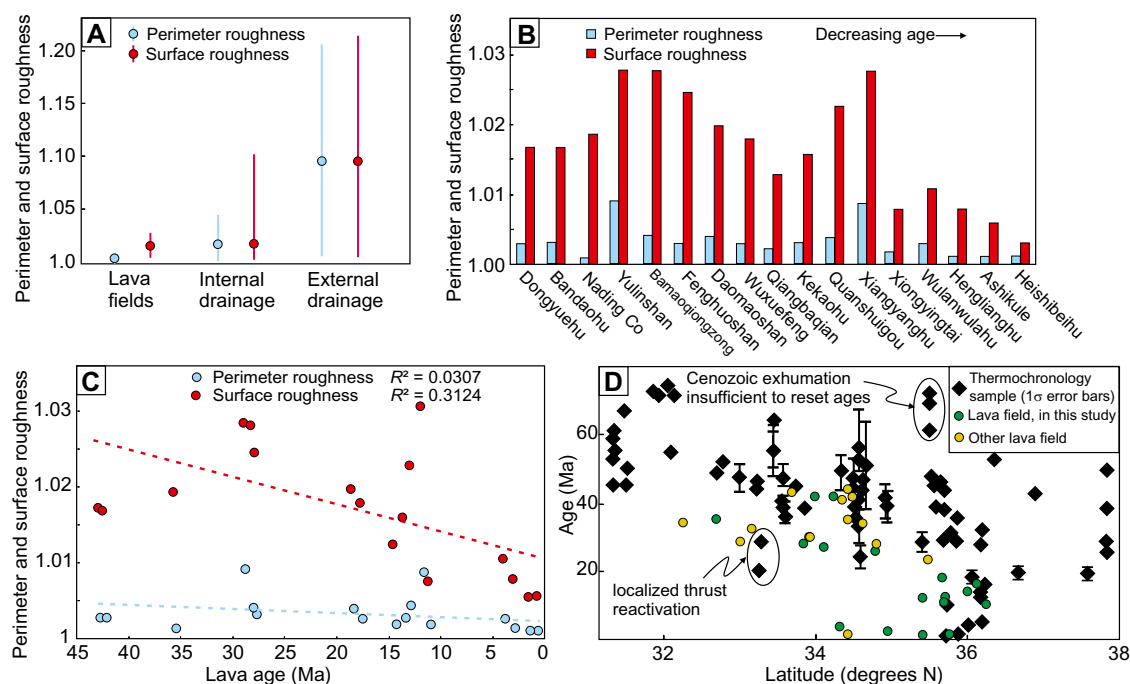


**Figure 3.** (A) Overall perimeter surface roughness values for Tibetan Plateau lava fields compared with test areas from internally drained and externally drained areas of the Tibetan Plateau. (B) Perimeter and surface roughness values for individual lava fields, ordered by decreasing field age. (C) Perimeter and surface roughness values for Tibetan Plateau lava fields versus lava ages. (D) Lava field ages and low-temperature thermochronology ages (Rohrmann et al., 2012; McRivette et al., 2019, and references therein) versus latitude. Caveats on thermochronology data outliers are from Rohrmann et al. (2012). Data sources are listed in Table DR1 (see footnote 1).

value to the internally drained regions of the plateau (averages 1.017 [1.028/1.006] and 1.018 [1.101/1.004]), and both groups are distinct from modern externally drained regions (average 1.095 [1.211/1.006]) (Fig. 3A). There is no relationship between PR and lava age (Fig. 3C; Table DR1). SR shows a gradual linear decrease with age (~0.003 every 10 m.y.), with a low  $R^2$  value (0.3124). Folded fields, Xiangyanghu and Yulinshan, have high PR and SR values (Fig. 3B).

Lava ages are plotted by latitude in Figure 3D. Qiangtang terrane lavas are typically ca. 40–25 Ma, although Pliocene flows are also present (Table DR1). Songpan–Ganzi terrane flows are typically  $\leq$  18 Ma. Published low-temperature thermochronology ages are also shown on Figure 3D. There is a ~20–30 m.y. difference between the oldest low-temperature thermochronologic ages (Rohrmann et al., 2012) and the oldest lava eruption ages at each latitude. The youngest thermochronology ages for each latitude overlap with the oldest eruption ages.

## DISCUSSION

There has been little erosion of the lava flows post-eruption, such that Paleogene lavas show remarkably similar morphologies to Neogene and Quaternary counterparts 20–30 m.y. younger (Fig. 3C). The decrease in SR value with decreasing age can be expected as gradual erosion occurs over tens of millions of years, though the very slow decrease shows that erosion within the Tibetan Plateau has been extremely limited within the internally drained area where these lavas are concentrated. The existence of undeformed and undissected ca. 40 Ma flows in the plateau interior indicates minimal long-term post-eruption erosion.

Thermochronology data show low erosional exhumation rates ( $<0.05$  mm/yr) across much of central Tibet after 45 Ma (Rohrmann et al., 2012), but give no direct information about contemporary relief. Lava eruption ages constrain the minimum age of the formation of low relief, given that the lava fields seal underlying landscapes comparable to the modern plateau (Fig. 3A). This study quantifies the time scales involved in the creation of regional plateau landscape, combining the distributions of lava-field ages and thermochronology data. Lava eruption ages in each area overlap the younger range of thermochronology ages (Fig. 3D). Plateau landscapes formed without a distinct time lag after the end of significant exhumation. The northward decrease in both lava ages and thermochronology ages (Fig. 3D) indicates that plateau landscape formation migrated northward between ~32.5°N and ~36.5°N from ca. 40 to ca. 10 Ma, equivalent to a long-term rate of ~15 km/m.y. for the diachronous development of the plateau landscape.

Our results do not indicate that the relief of the Tibetan Plateau interior is a consequence of

rifting (Wang et al., 2014), because the Neogene onset of extension (ca. 15–10 Ma) post-dates the older flows in central Tibet. Nor is there evidence of regionally simultaneous uplift and plateau growth in the late Miocene (Molnar et al., 1993). Progressive crustal thickening since the Eocene is a viable mechanism for both surface uplift and plateau landscape development (Fig. 2B). While crustal shortening via thrusting and folding is the most obvious way to achieve such thickening, lower-crustal flow would achieve the same result, and has been invoked in the northern Tibetan Plateau to explain an apparent shortfall in crustal shortening estimates (Staisch et al., 2016). Magmatism postdated plateau landscape creation, without significant later exhumation and/or major erosion. There is no indication of distinct time steps in the plateau landscape evolution, as might be expected if tectonic growth was stepwise (Fig. 2A; Tapponnier et al., 2001). If any of mantle lithosphere delamination (Fig. 2C; England and Houseman, 1989), lower-crustal flow (Fig. 2D; Clark and Royden, 2000), or magmatic underplating (Fig. 2C; Chen et al., 2018) took place after lava eruptions, they did so without leaving an imprint on the Cenozoic landscape record in the interior of the Tibetan Plateau.

## CONCLUSIONS

We have conducted a quantitative geomorphic study of Cenozoic lavas across the central and northern Tibetan Plateau. These lavas are typically undeformed, and were erupted over landscapes with relief similar to that of the modern plateau interior (Fig. 3A). Such low relief indicates that erosion and truncation of underlying, deformed rocks had taken place by the time of eruption. Preservation of lava fields for tens of millions of years suggests that they have lain within internally drained regions since eruption, without major erosion (Fig. 3C). Geomorphology results are combined with published lava ages and thermochronology data to show an overlap between the youngest exhumation ages and the oldest lava ages for each area (Fig. 3D). We therefore interpret plateau landscape formation to overlap the end of significant exhumation in each area. This process advanced northwards between ~32.5°N and ~36.5°N from ca. 40 to ca. 10 Ma at an average long-term rate of ~15 km/m.y. The simplest explanation of the results is that plateau growth is primarily a function of diachronous crustal thickening and surface uplift via isostasy (Figs. 2B and 2D), followed by creation of low relief and internally drained landscapes.

## ACKNOWLEDGMENTS

We thank Alexander Rohrmann for help compiling thermochronology data. Allen acknowledges the UK Natural Environment Research Council, grant NE/H021620/1. We thank Paul Kapp, Nathan Niemi, and two anonymous reviewers for helpful comments.

## REFERENCES CITED

- Chapman, J.B., and Kapp, P., 2017, Tibetan magmatism database: Geochemistry Geophysics Geosystems, v. 18, p. 4229–4234, <https://doi.org/10.1002/2017GC007217>.
- Chen, J.L., Yin, A., Xu, J.F., Dong, Y.H., and Kang, Z.Q., 2018, Late Cenozoic magmatic inflation, crustal thickening, and >2 km of surface uplift in central Tibet: *Geology*, v. 46, p. 19–22, <https://doi.org/10.1130/G39699.1>.
- Chung, S.L., Chu, M.F., Zhang, Y.Q., Xie, Y.W., Lo, C.H., Lee, T.Y., Lan, C.Y., Li, X.H., Zhang, Q., and Wang, Y.Z., 2005, Tibetan tectonic evolution inferred from spatial and temporal variations in post-collisional magmatism: *Earth-Science Reviews*, v. 68, p. 173–196, <https://doi.org/10.1016/j.earscirev.2004.05.001>.
- Clark, M.K., and Royden, L.H., 2000, Topographic ooze: Building the eastern margin of Tibet by lower crustal flow: *Geology*, v. 28, p. 703–706, [https://doi.org/10.1130/0091-7613\(2000\)28<703:TOBT EM>2.0.CO;2](https://doi.org/10.1130/0091-7613(2000)28<703:TOBT EM>2.0.CO;2).
- Ding, L., Kapp, P., Zhong, D.L., and Deng, W.M., 2003, Cenozoic volcanism in Tibet: Evidence for a transition from oceanic to continental subduction: *Journal of Petrology*, v. 44, p. 1833–1865, <https://doi.org/10.1093/petrology/egg061>.
- Ding, L., Kapp, P., Yue, Y.H., and Lai, Q.Z., 2007, Postcollisional calc-alkaline lavas and xenoliths from the southern Qiangtang terrane, central Tibet: *Earth and Planetary Science Letters*, v. 254, p. 28–38, <https://doi.org/10.1016/j.epsl.2006.11.019>.
- England, P., and Houseman, G., 1986, Finite strain calculations of continental deformation: 2. Comparison with the India-Asia collision zone: *Journal of Geophysical Research*, v. 91, p. 3664–3676, <https://doi.org/10.1029/JB091iB03p03664>.
- England, P., and Houseman, G., 1989, Extension during continental convergence, with application to the Tibetan plateau: *Journal of Geophysical Research*, v. 94, p. 17,561–17,579, <https://doi.org/10.1029/JB094iB12p17561>.
- Guo, Z.F., Wilson, M., Liu, J.Q., and Mao, Q., 2006, Post-collisional, potassic and ultrapotassic magmatism of the northern Tibetan Plateau: Constraints on characteristics of the mantle source, geodynamic setting and uplift mechanisms: *Journal of Petrology*, v. 47, p. 1177–1220, <https://doi.org/10.1093/petrology/egl007>.
- Guo, Z.F., and Wilson, M., 2019, Late Oligocene–early Miocene transformation of postcollisional magmatism in Tibet: *Geology*, v. 47, p. 776–780, <https://doi.org/10.1130/G46147.1>.
- Jolivet, M., Brunel, M., Seward, D., Xu, Z., Yang, J., Roger, F., Tapponnier, P., Malavieille, J., Arnaud, N., and Wu, C., 2001, Mesozoic and Cenozoic tectonics of the northern edge of the Tibetan plateau: Fission-track constraints: *Tectonophysics*, v. 343, p. 111–134, [https://doi.org/10.1016/S0040-1951\(01\)00196-2](https://doi.org/10.1016/S0040-1951(01)00196-2).
- Kapp, P., and DeCelles, P.G., 2019, Mesozoic–Cenozoic geological evolution of the Himalayan–Tibetan orogen and working tectonic hypotheses: *American Journal of Science*, v. 319, p. 159–254, <https://doi.org/10.2475/03.2019.01>.
- Liu, D.L., Li, H.B., Sun, Z.M., Pan, J.W., Wang, M., Wang, H., and Chevalier, M.-L., 2017, AFT dating constrains the Cenozoic uplift of the Qimen Tagh Mountains, Northeast Tibetan Plateau: Comparison with LA-ICPMS zircon U–Pb ages: *Gondwana Research*, v. 41, p. 438–450, <https://doi.org/10.1016/j.gr.2015.10.008>.
- McRivette, M.W., Yin, A., Chen, X.H., and Gehrels, G.E., 2019, Cenozoic basin evolution of the central Tibetan plateau as constrained by

- U-Pb detrital zircon geochronology, sandstone petrology, and fission-track thermochronology: *Tectonophysics*, v. 751, p. 150–179, <https://doi.org/10.1016/j.tecto.2018.12.015>.
- Molnar, P., England, P., and Martinod, J., 1993, Mantle dynamics, uplift of the Tibetan Plateau, and the Indian Monsoon: *Reviews of Geophysics*, v. 31, p. 357–396, <https://doi.org/10.1029/93RG02030>.
- Ozacar, A.A., and Beck, S.L., 2004, The 2002 Denali fault and 2001 Kunlun fault earthquakes: Complex rupture processes of two large strike-slip events: *Bulletin of the Seismological Society of America*, v. 94, p. S278–S292, <https://doi.org/10.1785/0120040604>.
- Rohrmann, A., Kapp, P., Carrapa, B., Reiners, P.W., Gynn, J., Ding, L., and Heizler, M., 2012, Thermochronologic evidence for plateau formation in central Tibet by 45 Ma: *Geology*, v. 40, p. 187–190, <https://doi.org/10.1130/G32530.1>.
- Rowley, D.B., and Currie, B.S., 2006, Palaeo-altimetry of the late Eocene to Miocene Lunpola basin, central Tibet: *Nature*, v. 439, p. 677–681, <https://doi.org/10.1038/nature04506>.
- Staisch, L.M., Niemi, N.A., Clark, M.K., and Chang, H., 2016, Eocene to late Oligocene history of crustal shortening within the Hoh Xil Basin and implications for the uplift history of the northern Tibetan Plateau: *Tectonics*, v. 35, p. 862–895, <https://doi.org/10.1002/2015TC003972>.
- Tapponnier, P., Xu, Z.Q., Roger, F., Meyer, B., Arnaud, N., Wittlinger, G., and Yang, J.S., 2001, Oblique stepwise rise and growth of the Tibet plateau: *Science*, v. 294, p. 1671–1677, <https://doi.org/10.1126/science.105978>.
- Taylor, M., and Yin, A., 2009, Active structures of the Himalayan-Tibetan orogen and their relationships to earthquake distribution, contemporary strain field, and Cenozoic volcanism: *Geosphere*, v. 5, p. 199–214, <https://doi.org/10.1130/GES00217.1>.
- Wang, C.S., Zhao, X.X., Liu, Z.F., Lippert, P.C., Graham, S.A., Coe, R.S., Yi, H.S., Zhu, L.D., Liu, S., and Li, Y.L., 2008, Constraints on the early uplift history of the Tibetan Plateau: *Proceedings of the National Academy of Sciences of the United States of America*, v. 105, p. 4987–4992, <https://doi.org/10.1073/pnas.0703595105>.
- Wang, C.S., Dai, J.G., Zhao, X.X., Li, Y.L., Graham, S.A., He, D.F., Ran, B., and Meng, J., 2014, Outward-growth of the Tibetan Plateau during the Cenozoic: A review: *Tectonophysics*, v. 621, p. 1–43, <https://doi.org/10.1016/j.tecto.2014.01.036>.
- Wang, Q., et al., 2016, Pliocene-Quaternary crustal melting in central and northern Tibet and insights into crustal flow: *Nature Communications*, v. 7, 11888, <https://doi.org/10.1038/ncomms11888>.
- Wu, Z.H., Barosh, P.J., Wu, Z.H., Hu, D.G., Xun, Z., and Ye, P.S., 2008, Vast early Miocene lakes of the central Tibetan Plateau: *Geological Society of America Bulletin*, v. 120, p. 1326–1337, <https://doi.org/10.1130/B26043.1>.
- Yakovlev, P.V., Saal, A., Clark, M.K., Hong, C., Niemi, N.A., and Mallick, S., 2019, The geochemistry of Tibetan lavas: Spatial and temporal relationships, tectonic links and geodynamic implications: *Earth and Planetary Science Letters*, v. 520, p. 115–126, <https://doi.org/10.1016/j.epsl.2019.04.032>.
- Yin, A., and Harrison, T.M., 2000, Geologic evolution of the Himalayan-Tibetan orogen: *Annual Review of Earth and Planetary Sciences*, v. 28, p. 211–280, <https://doi.org/10.1146/annurev.earth.28.1.211>.

Printed in USA